Computers and Concrete, Vol. 6, No. 2 (2009) 95-108
DOI: http://dx.doi.org/10.12989/cac.2009.6.2.095

Displacement-based seismic design of reinforced concrete columns strengthened by FRP jackets using a nonlinear flexural model

Chang-Geun Cho†

School of Architecture, Chosun University, Gwangju, Korea

Hee-Cheon Yun‡ and Yun-Yong Kim‡†

Department of Civil Engineering, Chungnam National University, Daejeon, Korea
(Received December 12, 2008, Accepted March 12, 2009)

Abstract. In the current research, a displacement-based seismic design scheme to retrofit reinforced concrete columns using FRP composite materials has been proposed. An accurate prediction for the nonlinear flexural analysis of FRP jacketed concrete members has been presented under multiaxial constitutive laws of concrete and composite materials. Through modification of the displacement coefficient method (DCM) and the direct displacement-based design method (DDM) of reinforced concrete structures, two algorithms for a performance-based seismic retrofit design of reinforced concrete columns with a FRP jacket have been newly introduced. From applications to retrofit design it is known that two methods are easy to apply in retrofit design and the DCM procedure underestimates the target displacement to compare with the DDM procedure.

Keywords: displacement-based design; nonlinear flexural model; concrete column; FRP jacket; multi-axial constitutive law; seismic retrofit.

1. Introduction

Over the past decade, several methods for performance-based design and evaluation of concrete or steel structures have been introduced in efforts to allow for the construction of longer and higher structures in seismic regions. The capacity spectrum method was first introduced by Freeman (1975, 1998). This procedure is to find the performance level by using the demand and capacity curves. The intersection of the two curves approximates the response of the structure. The displacement coefficient method used in the FEMA-273 (1996) is to estimate the target displacement by applying displacement coefficients and the initial stiffness of the structure. Direct displacement-based design concept introduced by Kowalsky *et al*. (1995) is to estimate the seismic performance of an inelastic single-degree-of freedom system representing the first mode of vibration of the multi-degree-of freedom system in which the nonlinear system is replaced by an equivalent linear system. This

† Assistant Professor, E-mail: chocg@chosun.ac.kr
‡ Assistant Professor
‡† Assistant Professor, Corresponding author, E-mail: yunkim@cnu.ac.kr

method was also applied to seismic design of unbonded post-tensioned masonry walls (Wight, *et al.*, 2007). By Chopra and Goel (2001), the direct displacement-based design was extended to estimate more rationally the performance of the structure.

On the other hands, it is well known that fiber reinforced polymer (FRP) can improve the strength and ductility of concrete by providing confinement (Mirmiran, 1997; Kawashima, 1997; Shahawy, *et al.*, 1995). A number of models for enhanced strength and ductility of confined concrete wrapped by FRP jackets were studied (Saadatmanesh, *et al.*, 1996; Samaan, *et al.*, 1998; Fam, *et al.*, 2001). A multiaxial constitutive model of FRP wrapped concrete was also initially applied in the prediction of axial compressive cylinders and flexural beam members (Cho, *et al.*, 2005; 2008).

The purpose of current study is to develop a procedure for realizing a performance-based seismic retrofit design of reinforced concrete columns strengthened by FRP jackets. For the seismic retrofit design, an algorithm of the direct displacement-based design method proposed by Chopra and Goel (2001) has been extended to determine the design thickness of the FRP jacket, and the retrofit design is also compared with the displacement coefficient method (FEMA-273, 1997).

2. Displacement coefficient method

According to the displacement coefficient method of FEMA-273 (1997), the target displacement, which is the maximum displacement occurring at the top of structures during a given earthquake, can be determined as

$$\delta_t = C_0 C_1 C_2 C_3 S_a \frac{T_e^2}{4\pi^2} g \tag{1}$$

where C_0 is the difference in displacement between the control node of multi-degree-of-freedom (MDOF) buildings and equivalent single-degree-of-freedom (SDOF) systems, C_1 is the modification factor for estimating the maximum inelastic deformation of SDOF systems from their maximum elastic deformation, C_2 is the response to possible degradation of stiffness and energy dissipation capacity for structural members during earthquakes, C_3 is the modification factor for including the P-Δ effects, T_e is the effective period of the evaluated structure, S_a is the spectral value of the acceleration response corresponding to T_e, and g is the ground acceleration (FEMA-273, 1997).

In Eq. (1), C_0 was derived from the participation factor of the first mode of the structure and C_1 was determined from the following equation.

$$\begin{aligned} C_1 &= 1.0, \ T_e \geq T_o \\ C_1 &= \frac{1.0 + (R-1)T_o/T_e}{R}, \ T_e < T_o \end{aligned} \tag{2}$$

where T_o is the characteristic period of ground motions and R is the ratio of required elastic strength to yield strength of structures. R can be determined as follows:

$$R = \frac{S_a}{V_y/WC_o} \frac{1}{} \tag{3}$$

where V_y is the yield base shear derived from a pushover analysis, as shown in Fig. 1, and W is the weight of the structure. Table 1 presents the values of C_2. Stiffness and strength degradation readily occur in structures that have properties of short period and low strength. With regard to C_3, when

the ratio of the post yield stiffness α is positive, C_3=1.0. Otherwise, the following equation should be used.

$$C_3 = 1.0 + \frac{|\alpha|(R-1)^{3/2}}{T_e} \tag{4}$$

Table 1. Modification Factor of C_2 (FEMA-273, 1997)

Performance level	T_e = 0.1sec	T_e^3 T_0 sec
Immediate occupancy	1.0	1.0
Life Safety	1.3	1.1
Collapse prevention	1.5	1.2

3. Direct displacement-based design method

3.1. Equivalent linear system

Needed in existing displacement-based design procedures, the properties of the equivalent linear system are summarized here. Consider an inelastic SDOF system with a bilinear force-displacement relationship on initial loading, as shown in Fig. 1. The stiffness of the elastic branch is k_o and that of the yielding branch is αk_o. The yield force and yield displacement are denoted by V_y and Δ_y, respectively. If the peak displacement of the inelastic system is Δ_m, the ductility factor equals to $\mu = \Delta_m / \Delta_y$.

For the bilinear system in Fig. 1, the natural vibration period of the equivalent linear system with the secant stiffness k_{sec} becomes

$$T_{eq} = T_n \sqrt{\frac{\mu}{1 + \alpha\mu - \alpha}} \tag{5}$$

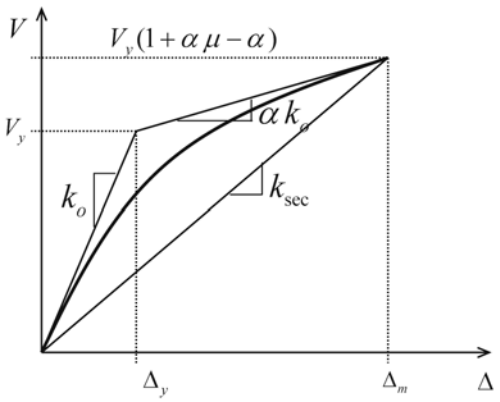

Fig. 1 Equivalent secant stiffness

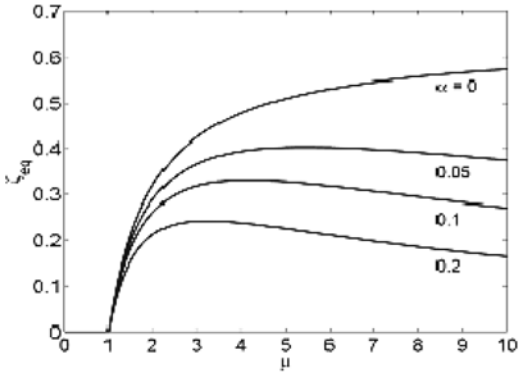

Fig. 2 Damping ratio vs. ductility factor (Chopra, *et al.*, 2001)

where T_n is the natural vibration period of the system vibrating within its linearly elastic range ($\Delta \leq \Delta_y$). The most common method for defining equivalent viscous damping is to equate the energy dissipated in a vibration cycle of an inelastic system and of an equivalent linear system. Based on this concept, as shown in Fig. 2, it can be shown that the equivalent viscous damping ratio is (Chopra and Goel, 2001):

$$\zeta_{eq} = \frac{2(\mu-1)(1-\alpha)}{\pi\mu(1+\alpha\mu-\alpha)} \tag{6}$$

The total viscous damping of the equivalent linear system is

$$\overline{\zeta}_{eq} = \zeta + \zeta_{eq} \tag{7}$$

where ζ is the viscous damping ratio of a bilinear system vibrating within its linearly elastic range ($\Delta \leq \Delta_y$). It should be noted that the bilinear assumption of restoring force is simple and practical but gives larger equivalent damping than the actual one in general for reinforced concrete members.

3.2. Design spectra

To implement the existing direct displacement-based design procedure, we have chosen to construct this spectrum by the procedures of Newmark and Hall (1982). The elastic design spectrum is illustrated in Fig. 3, where $\ddot{u}_{go}$, $\dot{u}_{go}$, and u_{go} are the peak values of the ground acceleration, velocity, and displacement, respectively, and their amplification factors are, respectively,

$$\alpha_A = 4.38 - 1.04\ln\zeta,\ \alpha_V = 3.38 - 0.67\ln\zeta,\ \alpha_D = 2.73 - 0.45\ln\zeta \tag{8}$$

where ζ is the damping ratio in percent.

Fig. 4 shows the Newmark-Hall displacement design spectra for several damping ratio values.

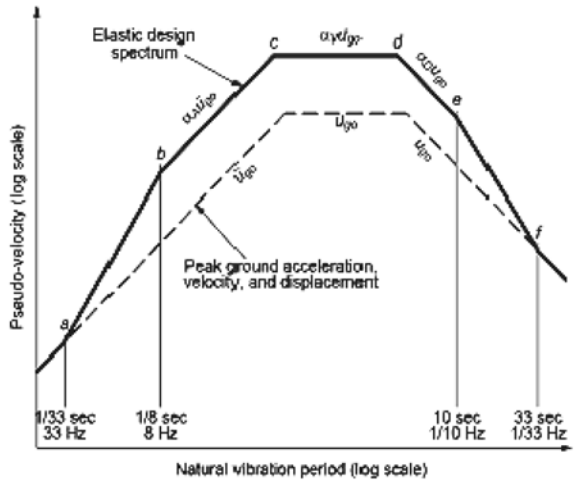

Fig. 3 Newmark-Hall design spectrum (Newmark, *et al.*, 1982)

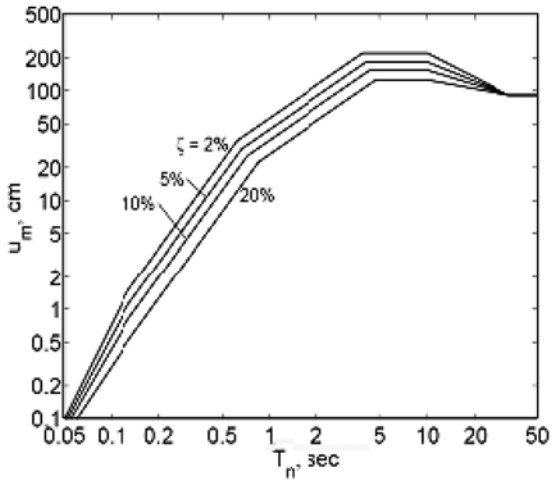

Fig. 4 Newmark-Hall displacement design spectrum (Chopra, *et al.*, 2001)

3.3. Direct displacement-based design procedure

Adapted from Priestley and Calvi (1997), a direct displacement-based design procedure for bilinear SDOF systems is outlined as a sequence of steps as follows (Chopra, *et al*., 2001):

1. Estimate the yield displacement Δ_y for the system.
2. Determine the acceptable plastic rotation θ_p of the hinge at the base.
3. Determine the design displacement Δ_m and design ductility factor $\mu = \Delta_m / \Delta_y$

$$\Delta_m = \Delta_y + \Delta_p = \Delta_y + \theta_P h \tag{9}$$

4. Estimate the total equivalent viscous damping $\overline{\zeta}_{eq}$ for the design ductility factor from Eqs. (6) and (7).
5. Enter the displacement design spectrum for elastic systems with known Δ_m and $\overline{\zeta}_{eq}$ to read T_{eq} from Fig. 4. Determine the secant stiffness

$$k_{\text{sec}} = \frac{4\pi^2}{T_n^2} M \tag{10}$$

where M is the mass of the system.

6. From Fig. 1, determine the required ultimate and yield forces, respectively

$$V_u = k_{\text{sec}} \times \Delta_m \tag{11}$$

$$V_y = \frac{k_{\text{sec}} \Delta_m}{1 + \alpha\mu - \alpha} \tag{12}$$

7. Estimate member sizes and detailing (FRP thickness) to provide V_y. Calculate the initial elastic stiffness k and $\Delta = V_y / k$.
8. Repeat steps 3 to 7 until a satisfactory solution is obtained.

4. Nonlinear flexural analysis of reinforced concrete members wrapped by FRP jackets

4.1. Stress-strain relation of FRP jacket and concrete wrapped by FRP jacket

Under the axial compressive behavior of concrete wrapped by FRP composites, as shown in Fig. 5, the strength and ductility of concrete depend on the confinement provided by the FRP jacket. In the figure, the behavior of the FRP jacket can be treated as the in-plane behavior of composite laminates, and from theory, the longitudinal and hoop strains of the FRP jacket can be expressed.

$$d\varepsilon_L = \frac{d\sigma_L}{E_L} - \nu_{LH}\frac{d\sigma_H}{E_H}, d\varepsilon_H = \frac{d\sigma_H}{E_H} - \nu_{LH}\frac{d\sigma_L}{E_L} \tag{13}$$

where $d\sigma_L$ and $d\sigma_H$ are the stress increment of the FRP jacket in the longitudinal and hoop direction, respectively; E_L and E_H are the elastic modulus of the FRP jacket in the longitudinal and hoop direction, respectively; and ν_{LH} is Poisson's ratio of the FRP jacket.

The strain and stress relationship of concrete, as shown in Fig. 6, can be treated as an orthotropic hypoelastic formulation in a multiaxial state according to the following incremental law

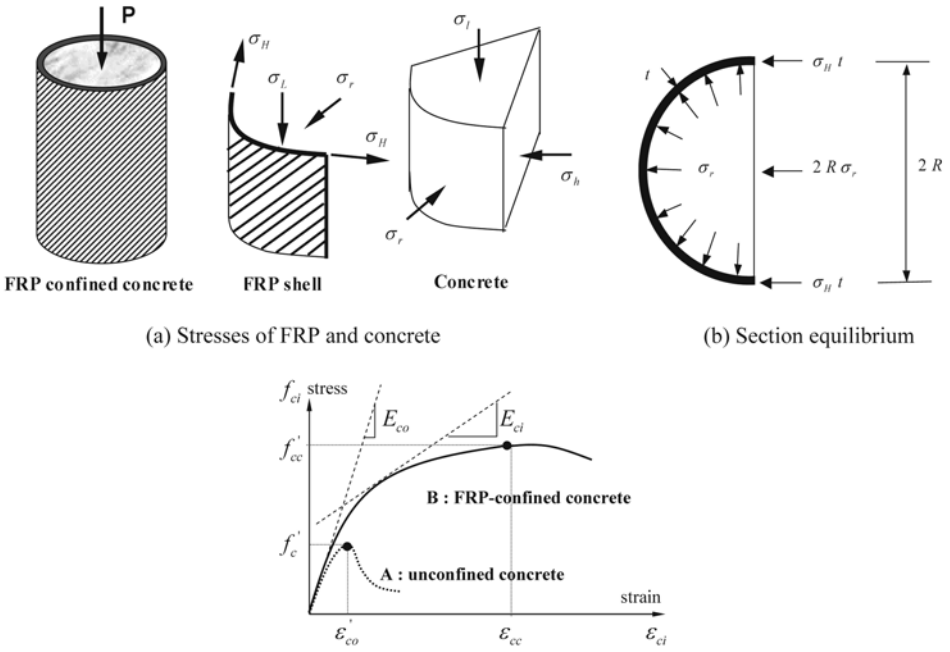

(a) Stresses of FRP and concrete

(b) Section equilibrium

(c) General stress-strain relationship of unconfined and FRP-confined concrete

Fig. 5 FRP-confined concrete under axial compression

$$\begin{Bmatrix} d\varepsilon_l \\ d\varepsilon_r \\ d\varepsilon_h \end{Bmatrix} = \begin{bmatrix} 1/E_l & -\mu_{lr}/\sqrt{E_l E_r} & -\mu_{lh}/\sqrt{E_l E_h} \\ & 1/E_r & -\mu_{rh}/\sqrt{E_r E_h} \\ sym. & & 1/E_h \end{bmatrix} \begin{Bmatrix} d\sigma_l \\ d\sigma_r \\ d\sigma_h \end{Bmatrix} \tag{14}$$

It can be assumed that the concrete properties in the radial direction are identical to those in the hoop direction, as $\sigma_r = \sigma_h$, $\varepsilon_r = \varepsilon_h$, $E_r = E_h$, $\mu_{lr} = \mu_{rh}$, and Eq. (14) becomes:

$$\begin{Bmatrix} d\sigma_l \\ d\sigma_r \end{Bmatrix} = \frac{1}{\Omega} \begin{bmatrix} E_l(1-\mu_{rh}^2) & 2\mu_{lr}\sqrt{E_l E_r}(1+\mu_{rh}) \\ \mu_{lr}\sqrt{E_l E_r}(1+\mu_{rh}) & E_r(1-\mu_{rh}) \end{bmatrix} \begin{Bmatrix} d\varepsilon_l \\ d\varepsilon_r \end{Bmatrix} \tag{15}$$

$$\Omega = 1 - 2\mu_{lr}^2(1+\mu_{rh}) - \mu_{rh}^2 \tag{16}$$

The equivalent uniaxial strain concept introduced by Darwin *et al.* (1977) has been used here to convert the two-dimensional coupled constitutive relations of Eq. (16) into two independent uniaxial constitutive relations. Here, if it is assumed that there is no slip between the concrete and the FRP shell, that is, the interfaces are perfectly bonded, the compatibility and equilibrium in the cross-section should be satisfied as $\varepsilon_L = \varepsilon_l$, $\varepsilon_H = \varepsilon_r$, and $\sigma_H = -\sigma_r R/t$, where R is the radius of the concrete core and t is the total thickness of the FRP shell. The longitudinal tangent modulus of the concrete E_l can be determined from the equivalent uniaxial stress and strain relationship of concrete, and the curve has been adopted from that proposed by Saenz (1964).

4.2. FRP-confined concrete in multiaxial stress states

The uniaxial stress-strain relation of unconfined and FRP-confined concrete is shown in Fig. 5. Since the behavior of concrete wrapped by a FRP shell is tri-axial rather than uniaxial, a tri-axial constitutive model is needed. To simulate such behavior and determine the compressive (peak) strength of FRP-confined concrete, the concrete failure surface proposed by Hsieh *et al.*(1979) has been applied to the stress state defined by σ_r, σ_h and σ_l, and the increased concrete compressive strength confined by the FRP shell can be expressed as

$$f'_{ci} = \lambda_{si} f_c' \tag{17}$$

where f_c' is the concrete uniaxial unconfined compressive strength. λ_{si} is the strength enhancement factor, defined as the ratio of confined to unconfined concrete strength, and can be determined from the failure surface proposed by Hsieh *et al.* (1979).

A strain failure surface is required to define the peak compressive strain ε'_{ci}, which becomes more ductile when the confinement is increased. The strain failure surface, however, is difficult to define directly from experiments. To account for the increased ductility, a strain enhancement factor λ_{ei} is introduced as

$$\varepsilon'_{ci} = \lambda_{ei} \varepsilon'_c \tag{18}$$

where ε'_{ci} is the maximum compressive strain of FRP-confined concrete, and ε'_c is the maximum uniaxial compressive strain of the unconfined concrete. In the current study, the factor λ_{ei} is determined based on experimental data available from biaxial, triaxial, and FRP-confined concrete (Kupfer, 1969; Mirmiran, 1997; Kawashima, 1997) with the relation of λ_{si} given as

$$\text{if } \lambda_{si} \leq 3 \quad \lambda_{ei} = 0.6 + 0.4(4\lambda_{si}^2 - 2\lambda_{si} - 1) \tag{19}$$

$$\text{if } \lambda_{si} > 3 \quad \lambda_{ei} = 5\lambda_{si} - 2.8 \tag{20}$$

To consider the influence of the state of stress on the process of dilation due to damage accumulation, the equivalent Poisson's ratio, taken as a cubic polynomial function, has been adopted with the correlation of biaxial and triaxial tests of concrete (Kupfer, *et al.*, 1969; Mills, *et al.*, 1970).

The incremental procedure for FRP-confined concrete under axial compression can be based on the FRP equivalent material properties and concrete stress-strain relation. Note that the number of shell layers, the direction of each layer, the layer stiffness, and the layer thickness are accounted for in the calculation of the equivalent material properties of the FRP laminate. For the prediction of the failure of the specimen, it is commonly accepted that the failure of concrete wrapped by a FRP shell is caused by the failure of the FRP composite materials. In the proposed model, the Tsai-Wu tensor failure criterion (1971) for composite materials has been adopted. After reaching the failure of the FRP shell in a section, it is assumed that the specimen cannot take any additional loads.

5. Flexural model of reinforced concrete member wrapped by FRP jacket

Based on the axial compressive model of FRP-confined concrete, an analysis procedure for

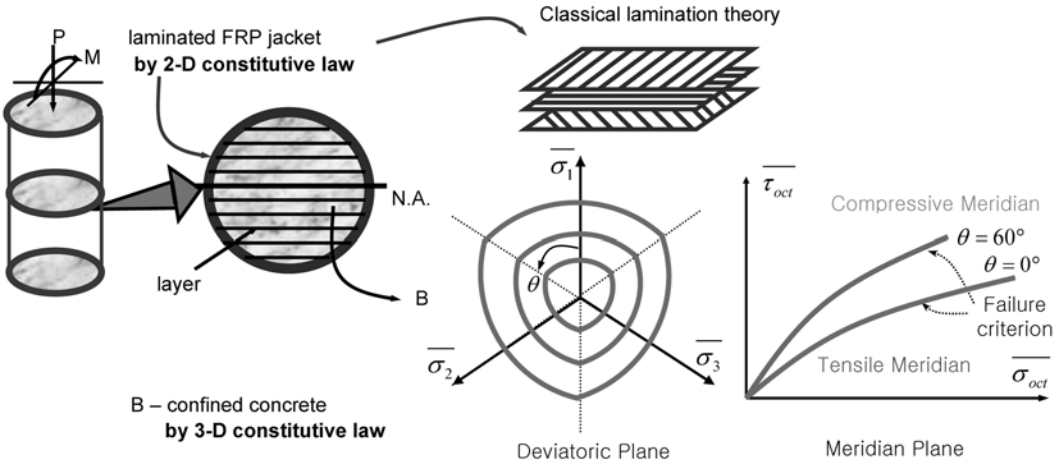

Fig. 6 Flexural analysis of FRP-confined concrete members (Cho, *et al.*, 2008)

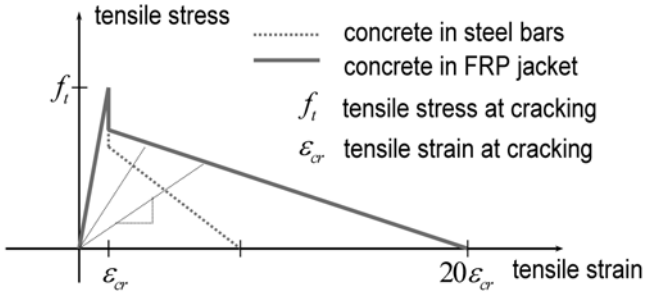

Fig. 7 Tensile behavior of FRP-confined concrete (Shahawy, *et al.*, 1995)

flexural behavior of reinforced concrete members wrapped by a FRP composite jacket has been proposed, as shown in Fig. 6, using a layer approach for the nonlinear cross-section analysis.

When modeling concrete under tension, it is assumed that the response is linear elastic in the pre-cracked region and, after concrete cracks, tension stiffening occurs in concrete reinforced with steel bars or a composite jacket. Tests by Shahawy and Beitelman (1995) indicate that an FRP layer combined with steel bars generates a greater tension stiffening effect in concrete compared to steel bars alone, because it is directly attached to a large surface area in concrete, as shown in Fig. 7. Tension stiffening due to the FRP layer combined with steel bars can be expressed as a linear degradation from 70% of the tensile stress at cracking to zero at a strain 20 times the tensile strain at cracking. Based on the experimental results, it is assumed in the proposed model that tension stiffening due to the FRP layer alone degrades the tensile stress to zero at a strain 15 times the tensile strain at cracking.

At each loading stage, the FRP jacket is checked for failure by Tsai-Wu criteria (1971) and the failure of the member is assumed when the FRP jacket reaches failure. The detailed algorithm of the nonlinear analysis procedure is presented in Fig. 8.

The current analytical model was compared with several experiments of FRP-wrapped concrete both on axial compressive cylinders and flexural beams (Cho, *et al.*, 2005; 2008), and the predicted results were well estimated the experimental results.

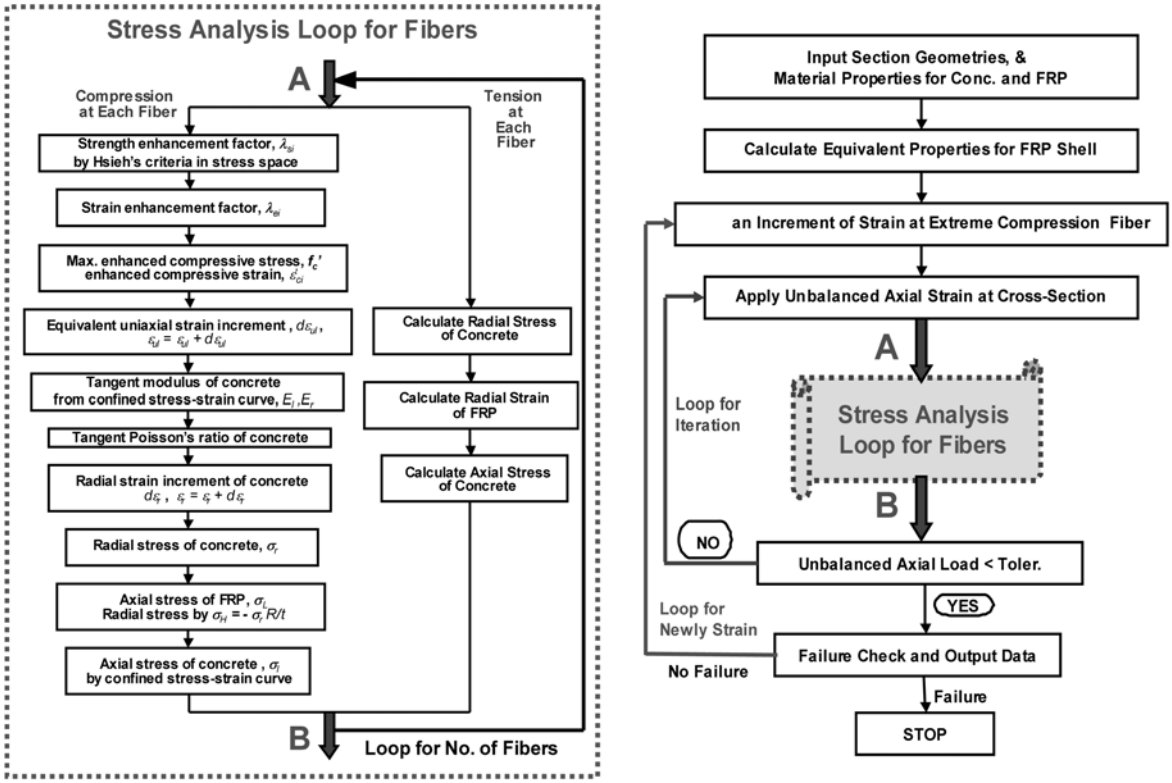

Fig. 8 Algorithm of flexural analysis of FRP-confined concrete members

6. FRP jacket design

6.1. FRP Jacket design for flexural strength and ductility enhancement

From the required plastic rotation θ_p of the plastic hinge, the plastic curvature can be obtained with the following equation

$$\phi_p = \frac{\theta_p}{L_p} \tag{21}$$

where L_p is the plastic hinge length, given by Priestley *et al.* (1996)

$$L_p = g_j + 0.044 d_{lb} f_{yl} \tag{22}$$

where g_j is the gap between the jacket and the footing, f_{yl} is the expected yield stress of reinforcing steel, and d_{lb} is the diameter of longitudinal bar.

The effective volumetric ratio of retrofit material for a circular FRP jacket of diameter D becomes

$$\rho_j = \frac{4t_j}{D} \tag{23}$$

A conservative estimate for the ultimate compression strain of circular columns retrofitted with

FRP jackets is given by (Priestely, *et al*., 1996)

$$\varepsilon_{cu} = 0.004 + \frac{2.5\rho_j f_{uj}\varepsilon_{uj}}{f_{cc}'} \tag{24}$$

where f_{uj} and ε_{uj} are the ultimate stress and strain of the FRP jacket material. From Eq. (23) and (24), the required jacket thickness can be determined as

$$t_j = \frac{0.1(\varepsilon_{cu} - 0.004)Df_{cc}'}{f_{uj}\varepsilon_{uj}} \tag{25}$$

6.2. FRP Jacket design for shear strength and shear strength enhancement

Since the costs of retrofitting columns for shear strength will not be greatly affected by jacket thickness, it is appropriate to adopt the same conservatism for retrofit shear design as for new design. Hence, the design shear force should be based on conservatively high estimates of column plastic hinge flexural of shear strength, in accordance with recommendations. The additional shear strength required to be imparted by the column retrofit can therefore be given as

$$\phi_s V_{sj} \geq V^o - \phi_s(V_c + V_{sh} + V_p) \tag{26}$$

where ϕ_s is the strength reduction factor for shear force, V^o is the maximum feasible shear force, V_{sj} is the additional shear strength imparted by membrane shear flow in the jacket, V_c is the shear strength by concrete portion, V_{sh} is the shear depending on transverse reinforcement by truss mechanism, and V_p is the shear strength provided by the axial compression in the column. The concrete shear strength can be expressed as

$$V_c = \alpha_c \beta k \sqrt{f_{ck}} A_e \tag{27}$$

where $1 \leq \alpha_c = \left(3 - \frac{M}{VD}\right) \leq 1.5$, $\beta = (0.5 + 20\rho_l) \leq 1$, $A_e = 0.8A_g$, and k, within plastic end regions, depends on the member displacement ductility factor, μ, as shown in Fig. 9.

The shear strength depending on transverse reinforcement by a truss mechanism for a circular

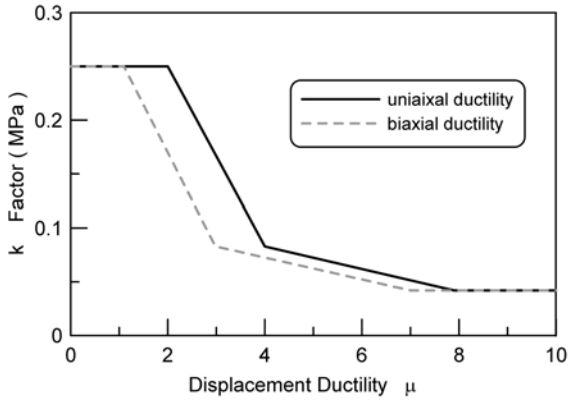

Fig. 9. Displacement ductility factor and shear strength reduction factor

column is given by

$$V_{sh} = \frac{\pi}{2}\frac{A_h f_{yh} D'}{s}\cot\theta \tag{28}$$

The shear strength enhanced from axial compression P is considered as an independent component of shear strength, resulting from a diagonal compression strut, and is given by

$$V_p = P \cdot \tan\gamma \tag{29}$$

For a cantilever column, γ is the angle formed between the column axis and the strut from the point of load application to the center of the flexural compression zone at the column plastic hinge critical section.

The shear strength of a circular passive FRP jacket is equivalent to the hoop reinforcement of area $A_h = t_j$ at a spacing of s=1, given by

$$V_{sj} = \frac{\pi}{2} t_j (0.004 E_j) D \cot\theta \tag{30}$$

By combining Eq. (26) and (30), the required thickness of the FRP jacket can be determined as

$$t_{j,req} \geq \frac{V^o / \phi_s - (V_c + V_{sh} + V_p)}{\frac{\pi}{2}(0.004 E_j) D \cot\theta} \tag{31}$$

7. Examples of retrofit design of circular columns

To evaluate the two procedures of displacement-based seismic retrofit design described in the previous chapters, a circular reinforced concrete column with a column height of H=5.486 m and a

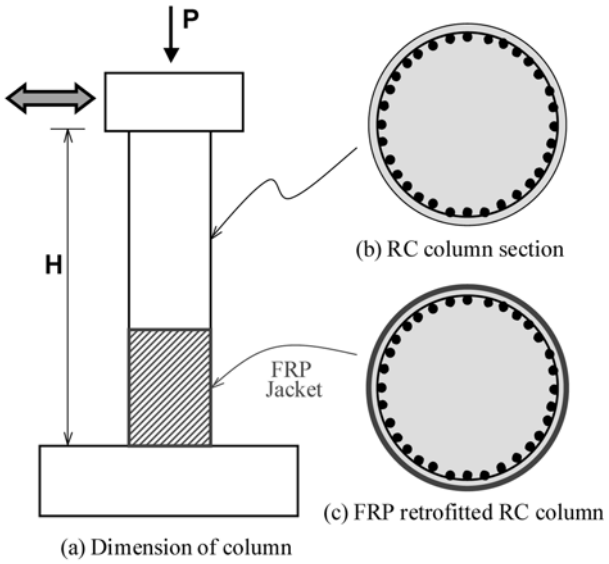

Fig. 10 Design example of a retrofit RC column

column diameter of 1.829 m, as shown in Fig. 10, was considered (Priestley, *et al*. 1996). Longitudinal reinforcement consists of 54 No. 14 (D43) bars of yield stress f_{yl}=345 MPa bundled in pairs, with transverse reinforcement No. 4 (D12.7) of yield stress f_{yh}=303 MPa at 305 mm centers. The constant axial load on the column is 5350 kN and the uniaxial compressive strength of concrete is f_c'=41.4 MPa. A carbon FRP composite jacket was applied as the retrofit material and the material characteristics of the CFRP jacket were an elastic modulus of E_j=82800 MPa and a failure strength of f_{uj}=1034 MPa.

The DDM procedure described in the previous section was implemented for a design example of the circular column described above. The given design earthquake load was set to a peak ground acceleration (PGA) of 0.8 g, and the CFRP composite jacket was to be designed for the column so as to enable it to sustain a targeted performance displacement of Δ_m=260 mm at its top. The monotonic load-displacement curve from a nonlinear pushover analysis of the reinforced concrete column (without retrofit) was obtained as shown in Fig. 11. For the reinforced concrete column, the yield displacement was estimated as Δ_y=18 mm with a corresponding yield load of 4100 kN and a total displacement of 88 mm with a ductility factor of 4.89. After retrofit design iterations of the column by the DDM procedure, the design thickness of jacket was determined as 12.0 mm. The load-displacement curve of the retrofitted column is shown in Fig. 12. After the final determination of the jacket thickness, the yield displacement of the retrofitted column was increased to 21.0 mm corresponding with a yield shear force of 4350 kN, and the total displacement of the retrofitted column was also increased to 260 mm with a ductility factor of 12.4. By applying the retrofit design of a column with a CFRP jacket with a thickness of 12.0 mm, the column was considerably enhanced in terms of load-carrying and deformation capacities.

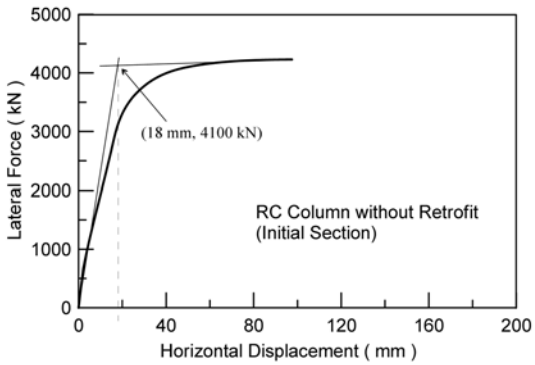

Fig. 11 Pushover curve of RC column

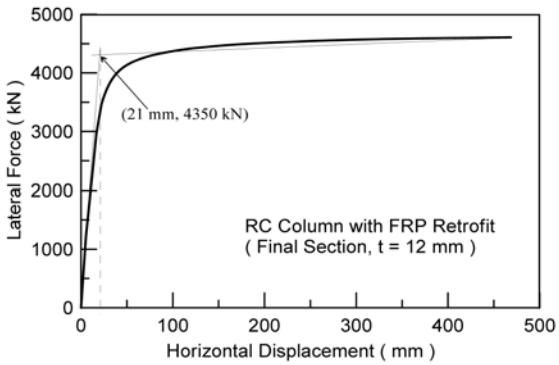

Fig. 12 Pushover curve of CFRP retrofit RC column

Table 2. Design results both by DCM and DDM

Design Parameters	RC column	Retrofitted RC column	
		DDM	DCM
Design thickness of CFRP jacket	-	12.0 mm	12.0 mm
Yield displacement	18 mm	21 mm	21 mm
Total displacement	88 mm	260 mm	127 mm
Ductility factor	4.89	12.4	6.0
Yield shear force	4100 kN	4350 kN	4350 kN

The column retrofitted with a CFRP jacket with a thickness of 12.0 mm was also evaluated with respect to seismic performance by the DCM procedure described in the previous section and the results were compared with those derived with the DDM procedure, as shown in Table 2. In the comparison with the DDM procedure, the DCM procedure underestimates the target displacement of the retrofitted column by 48.8% and the ductility factor by 48.4%. It is judged that the target displacement of the DCM procedure is determined from the initial stiffness of the pushover curve while that of the DDM procedure is determined from the secant stiffness of the nonlinear pushover curve.

8. Conclusions

Two displacement-based design procedures to retrofit concrete columns by FRP jackets have been introduced. In order to predict the nonlinear pushover curve of retrofitted columns, an accurate prediction for the nonlinear flexural analysis of FRP jacketed concrete members has been presented under multiaxial constitutive laws of concrete and composite materials. From applications of column retrofit design, it is found that the two design procedures is easy to apply in the practice of retrofit design and the DCM procedure underestimates the target displacement to compare with the DDM procedure.

References

Calvi, G.M. and Kingsley, G.R. (1997), "Displacement-based seismic design of multidegree-of-freedom bridge structures", *Earthq. Eng. Struct. Dyn.* **24**, 1247-1266.

Cho, C.G., Kwon, M. and Spacone, E. (2005), "Analytical model of concrete-filled fiber-reinforced polymer tubes based on multiaxial constitutive laws", *J. Struct. Eng.*, ASCE, **131**(9), 1426-1433.

Cho, C.G. and Kwon, M. (2008), "Prediction of nonlinear bending behavior for FRP concrete beams based on multi-axial constitutive laws", *Eng. Struct.*, **30**(9), 1311-2320.

Chopra. A.K. and Goel, R.K. (2001), "Direct displacement-based design: use of inelastic design spectra versus elastic design spectra", *Earthq. Spectra*, **17**(1), 47-64.

Fam, A.Z. and Rizkalla, S.H. (2001), "Confinement model for axially loaded concrete confined by circular fiber-reinforced polymer tubes", *ACI Struct. J.*, **98**(4), 451-461.

Federal Emergency Management Agency (FEMA) (1997), *NEHRP Guidelines for the Seismic Rehabilitation of Buildings*, Report FEMA 273 (Guidelines) and Report 274 (Commentary), Washington, D.C.

Freeman, S.A., Nicoletti, J.P. and Tyrell, J.V. (1975), "Evaluations of existing buildings for seismic risk, a case study of puget sound naval shipyard," *Proceedings of the 1st U.S. National Conf. on Earthquake Engineering*, Bremerton, Washington, 113-1220.

Freeman, S.A. (1998), "Development and use of capacity spectrum method", Paper No. 269, 6th US National Conference on Earthquake Engineering/EERI, Seattle, Washington.

Hsieh, S.S., Ting, E.C. and Chen, W.F. (1979), "An elastic-fracture model for concrete," *ASCE Proc. 3d Eng.* Mech. Div. Spec. Conf, 437-440.

Kawashima, K., Hosotani, M. and Hoshikuma, J. (1997), "A model for confinement effect for concrete cylinders confined by carbon fiber sheets", NCEER-NICEDE Workshop on Earthquake Engineering Frontiers in Transportation Facilities, NCEER, State Univ. of New York, Buffalo, N.Y.

Kowalsky, M.J., Priestley, M.J.N. and MacRae, G.A. (1995), "Displacement-based Seismic Design of RC Bridge Columns in Seismic Regions", *Earthq. Eng. Struct. Dyn.*, **24**, 1623-1643.

Kupfer, H. (1969), "Behavior of concrete under biaxial stress", *J. ACI*, **66**(8), 656-666.

Mills, L.L. and Zimmerman, R.M. (1970), "Compressive strength of plain concrete under multiaxial loading conditions", *J. ACI*, **67**(10), 802-807.
Mirmiran, A. and Shahawy, M. (1997), "Behavior of concrete columns confined by fiber composites", *J. Struct. Eng.*, ASCE, **123**(5), 583-590.
Newmark, N.M. and Hall, W.J. (1982), *Earthquake Spectra and Design*, EERI Monograph Series, Earthquake Engineering Research Institute, Oakland, California.
Priestley, M.J.N., Seible, F. and Calvi, G.M. (1996), *Seismic Design and Retrofit of Bridges*, John Wiley & Sons, New York.
Priestley, M.J.N. and Calvi, G.M. (1997), Concepts and procedures for direct displacement-based design, Seismic Design Methodologies for the Next Generation of Codes, Fajfar and Krawinkler (eds), Balkema, Rotterdam, 171-181.
Saadatmanesh, H., Ehsani, M.R. and Jin, L. (1996), "Seismic strengthening of circular bridge pier models with fiber composites" *ACI Struct. J.*, **93**, 639-647.
Saenz, L.P. (1964), "Discussion of equation for the stress-strain curve of concrete by desayi and krishman", *J. ACI*, **61**(9).
Samaan, M., Mirmiran, A., and Shahawy, M. (1998), "Model of concrete confined by fiber composites", *J. Struct. Eng.*, ASCE, **124**(9), 1025-1031.
Shahawy, M. and Beitelman, T.E. (1995), "Structural applications of advanced composite materials in bridge construction and repair", Proc. of the XIII ASCE Structures Congress.
Tsai, S.W, and Wu, E.M. (1971), "A general theory of strength for anisotropic materials", *J. Comp. Mater.* **5**, 58-80.
Wight, G.D., Kowalsky, M.J. and Ingham, J.M. (2007), "Direct displacement-based seismic design of unbonded post-tensioned masonry walls" *ACI Struct. J.*, **104**, 560-569.